ESKİŞEHİR TECHNICAL UNIVERSITY JOURNAL OF SCIENCE AND TECHNOLOGY
A- APPLIED SCIENCES AND ENGINEERING

2022, 23(4), pp. 244-255, DOI:10.18038/estubtda.1054195

APPLICATION OF HOOKE'S LAW TO ANGLE PLY LAMINA

Cagatay YILMAZ[1,*], Hafiz Qasim ALI [2], Mehmet YILDIZ [3]

[1*] Mechanical Engineering, Faculty of Engineering, Abdullah Gul University, Kayseri, Turkey
[2] Material Science and Nanoengineering, Faculty of Engineering and Natural Sciences, Sabancı University, Istanbul, Turkey
[3] Material Science and Nanoengineering, Faculty of Engineering and Natural Sciences, Sabancı University, Istanbul, Turkey

ABSTRACT

Aerospace-grade carbon fiber reinforced polymer composite plates with four different fiber orientations 0º, 30º, 45ºand 60º is produced with the autoclave curing method and subjected to tensile testing. The stress-strain curves of the composite specimens are compared with Hooke's law. It is observed that Hooke's law coincides precisely with the experimental results for samples containing fibers parallel to the loading direction. However, it does not coincide with samples where the fibers make a certain angle with the applied load direction. Moreover, it is reported that Hooke's law converges the experimental results for small strain values but diverges significantly from the experimental results at higher strain values.

Keywords: Hooke's law, Composite lamina, Tensile test, Angle ply lamina

1. INTRODUCTION

Laminated composites gained attention in major industries such as aerospace, defense, and automotive due to their versatile design, flexible manufacturing methods, and high strength-to-weight ratio. The usage of laminated composite makes the structure of the vehicle lighter and provides a longer range with the same amount of fuel. In order to use the laminated composite structure reliably within these industries, their modeling should be well understood and analyzed. If their modeling is well understood and precisely fits with the experimental finding, the need for mechanical characterization in the component development stage can be eliminated. The elimination of the mechanical characterization for laminated composite helps engineers to shorten component development time, thus reducing the costs.

Several experimental studies have been conducted to understand the experimental behavior of laminated composites [1–10], and finite element analyses are performed to simulate the behavior of laminated composites under certain loading conditions [11–13]. In addition to pure experimental or numerical studies, several studies present the correlation and validation to understand better the mechanical performance and failure behavior of the laminated composites[14–18].

A laminated composite can be modeled from two perspectives: micromechanics and macro mechanics. As per the micromechanics of a composite, a laminate consists of fiber and matrix. If the mechanical properties of fiber and matrix are known, then the whole laminate can be modeled by using these properties. In macro mechanics, a laminate is constructed from different laminae where each lamina can have a different fiber orientation. This difference in the orientation of fibers affects the mechanical properties of the laminate. The mechanical properties of laminate can be predicted by applying Hook's law to Classical Lamination Theory (CLT). CLT assumes that a laminate consists of different laminae and considers the angle of each lamina. It can be seen in the open literature that there are several studies that both use Hooke's law and CLT [19–22]. Since a laminate consists of several laminae, the application of Hooke's law should be well analyzed, validated, and understood in the lamina order.

*Corresponding Author: yilmaz.cagatay@agu.edu.tr
Received: 06.01.2022 Published: 29.12.2022

Hooke's law can be applied to lamina from a macro-mechanic perspective to explain the effect of varying fiber angles on stiffness in many textbooks [23–25]. These textbooks explain the application of Hooke's law for unidirectional and angle ply lamina and relate stress with strain. However, when the literature is investigated, it is seen that there is a lack of validation of Hooke's law with experimental data for angle ply composite lamina.

This research is an effort to fill the gap for a better understanding of whether Hook's law is confidently applicable for angle ply lamina or not. For that purpose, four different directions of carbon fiber reinforced polymeric lamina are produced through the autoclave curing method and then tested under tensile loading up to the failure point to acquire stress-strain data, which is then compared with Hooke's law.

2. MATERIALS AND METHODS

2.1. Materials and Sample Preparation

Carbon fiber prepreg, with a trading name of AX-6201XL-C, is obtained from Kordsa. The prepreg consists of unidirectional fibers with an aerial fiber weight of 300 gsm. Before laying up, the carbon fiber prepreg is cut with a dimension of 300x300 mm by using ZÜND G3-L3200 Digital Ply Cutter with desired fiber orientations. Four different composite plates are manufactured by an autoclave curing method. First, prepreg stacks are placed on a pre-treated steel plate with Axel Xtend 838 mold release agent. Two thermocouples (TC1 and TC 2) are attached to two different prepreg stacks with a heat-resistant tape called Flash Breaker. These thermocouples are used to monitor the temperature of prepreg stacks during autoclave curing. Prepreg stacks are covered with Airtech WL5200 release film, Airtech N10 breather fabric, and Airtech WL 7400 vacuum bag. The vacuum bag is sealed with Airtech AT 200Y sticky tape. Here, breather fabric is used for air evacuation inside the bagging, and release film prevents the sticking of breather fabric to prepreg stacks. Once the prepreg stacks are bagged, the vacuum leak test is performed for two minutes. At the end of the vacuum leak test, no vacuum leak is observed. Once every necessary step is completed for a secure autoclave run, a recipe is created in the autoclave software based on the prepreg manufacturer's recommendations. The autoclave is pressured with Nitrogen gas. The curing process parameters of four different prepreg stacks are depicted in Figure 1. Autoclave gage pressure (Pressure), autoclave temperature (AirTC), and part temperatures (TC1 and TC2) can be seen in Figure 1 (a), and the vacuum gage pressure inside the bag can be seen in Figure 1 (b).

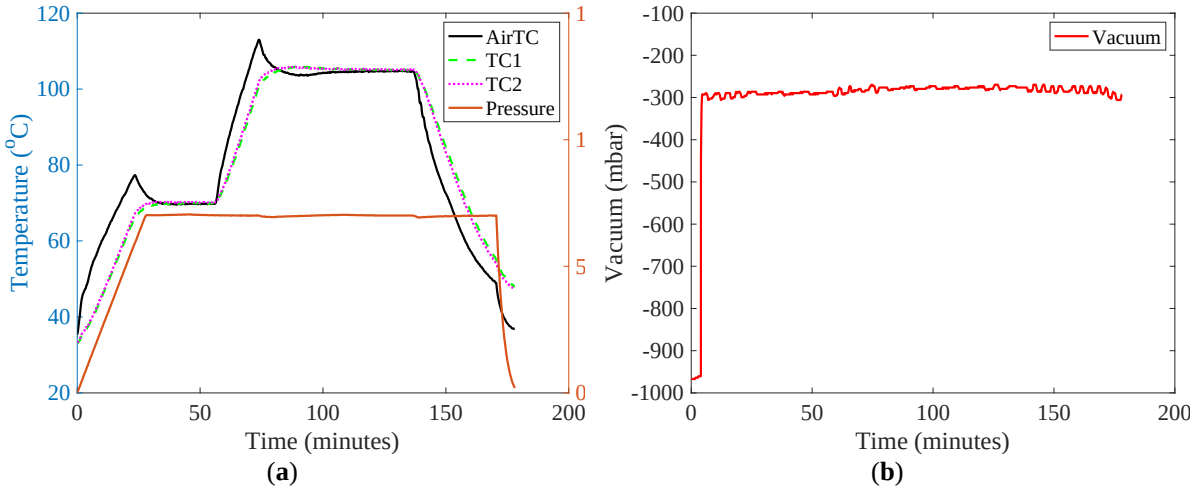

Figure 1. Curing condition for prepreg stack (a) Air temperature (AirTC), thermocouples attached to prepreg stacks (TC1 and TC2) and gauge pressure in the autoclave (Pressure), (b) gage vacuum inside the bagging

Once the autoclave cycle is completed, composite plates are carefully removed from the bagging materials. In order to prevent the composite plates from mixing with each other, the plates are immediately marked with their codes and fiber directions after they are cleared of the bag materials

A visual inspection is performed to check for any production imperfections. It is observed that composite plates are produced of good quality. The produced composite plates are then taken into dimensional quality inspection in order to check the homogeneity of thickness over the plates. It is seen that each composite plate has a homogeneous thickness of 1.2 mm. Once the quality of the composite plates is assured, they are sent to the tabbing station. The stacking sequence of composite plates and their codes along with their measured strength are given in Table 1.

Table 1. The configuration of plates and their code

Configuration	Code	Strength (MPa)
$[0]_4$	CY0	2112
$[30]_4$	CY30	70
$[45]_4$	CY45	58.6
$[60]_4$	CY60	41

The produced plates are tabbed with glass fiber reinforced polymer tabbing material for the tensile test. Glass fiber tabs are adhered to the produced test plate with 3M AF 163-2k adhesive film. The curing of the adhesive film is performed in a vacuum oven, and it is described in a previous publication [26]. First, the extraction of test coupons from the composite plates is attempted with the Poysan 3-axis router, and it is successful for the CY0, CY45, and CY60. However, it is seen that the CY30 test plate is so brittle that it is impossible to cut tensile test coupons with the router. Therefore, tensile test coupons from the CY30 plate are cut with a water jet (KUKA KR16 equipped with KMT Neoline 40i OEM water pressurizing system 3000 bar speed 250 mm/min). The tabbed tensile test coupons extracted from CY60 and CY0 test plates can be seen in Figure 2 (a &b), respectively. The dimensions of all test coupons are chosen per the ASTM D3039 standard and can be seen in Table 3.

2.2. Mechanical Testing

All mechanical tests are performed with a Universal Test Machine (UTM) (Instron 8803) equipped with a load cell of ±250 kN under the crosshead displacement of 2 mm/min. Axial strain data is recorded with a video extensometer (AVE 2.0), and transversal strain data is recorded with a mechanical extensometer (Epsilon 3542).

In order to analyze the reliability of Hooke's law for angle-ply lamina, material constants of the unidirectional lamina, namely, elastic modulus in the direction of fiber (E_{11}), elastic modulus in the perpendicular direction to fiber (E_{22}), the major Poisson's ratio, and in-plane shear modulus are needed. Among these material constants of the unidirectional lamina, E_{11}, E_{22}, and υ_{12}, are measured by applying the principles of ASTM D 3039 Standard Test Method for Tensile Properties of Polymer Matrix Composite Materials [27] and G_{12} is measured by following the ASTM D 3518 Standard Test Method for In-Plane Shear Response of Polymer Matrix Composite Materials by Tensile Test of a ±45° Laminate [28] standards. The material constant measured by following these standards is given in Table 2.

Table 2. Material constants of unidirectional lamina

Material constant	Value	Standard
E_{11}	128 GPa	ASTM D 3039
E_{22}	17.7 GPa	ASTM D 3039
υ_{12}	0.289	ASTM D 3039
G_{12}	14.4 GPa	ASTM D 3518

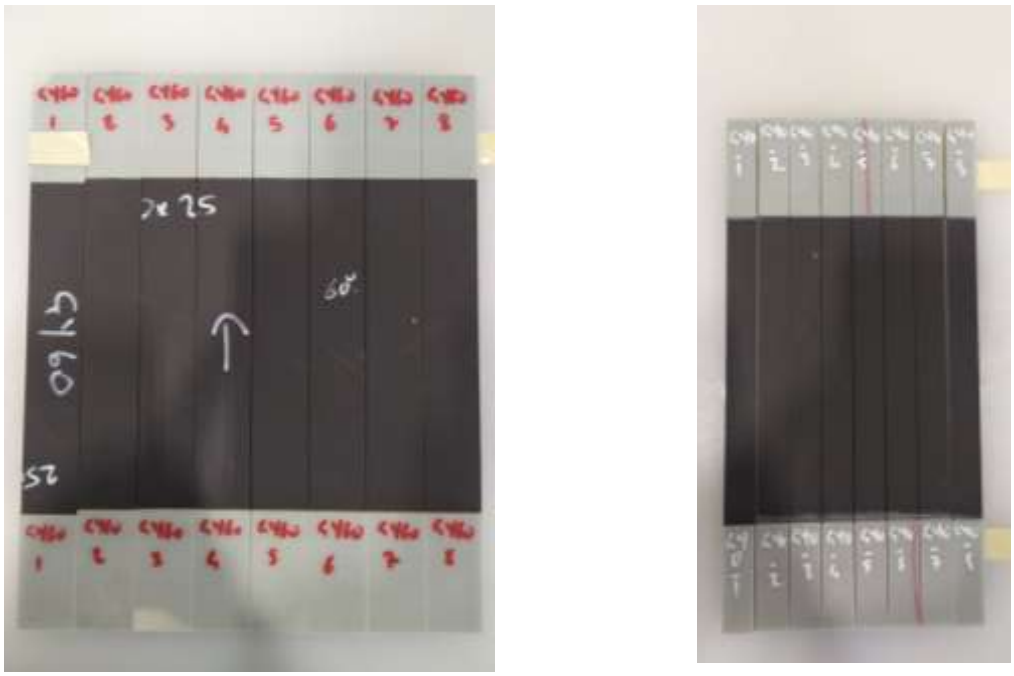

(a) (b)

Figure 2. Tensile test coupons ready to test, (a) CY60 coupons, (b) CY0 coupons

Table 3. Dimensions of coupons

Code	Gage length (mm)	Tab length (mm)	Width (mm)	Overall length (mm)
CY0	138	56	15	250
CY30	150	50	25	250
CY45	150	50	25	250
CY60	150	50	25	250

2.3. Hooke's Law

A plane stress assumption can be made if a thin plate experiences only in-plane loads. A thin plate has a relatively small thickness compared to its width and length. Therefore, a composite lamina can be treated as a thin plate. Under a plane stress assumption, three stress terms, σ_3, σ_{31}, σ_{23} are zero and the 3D stress-strain equation can be reduced to a 2D stress-strain equation. This two-dimensional stress-strain relation can be expressed with Equation (1)

$$\begin{bmatrix}\sigma_1\\ \sigma_2\\ \tau_{12}\end{bmatrix}=\begin{bmatrix}Q_{11} & Q_{12} & 0\\ Q_{12} & Q_{22} & 0\\ 0 & 0 & Q_{66}\end{bmatrix}\begin{bmatrix}\varepsilon_1\\ \varepsilon_2\\ \gamma_{12}\end{bmatrix} \quad (1)$$

In Equation (1), the direction of fibers is assumed as direction 1, while the direction perpendicular to fibers is referred to as direction 2.

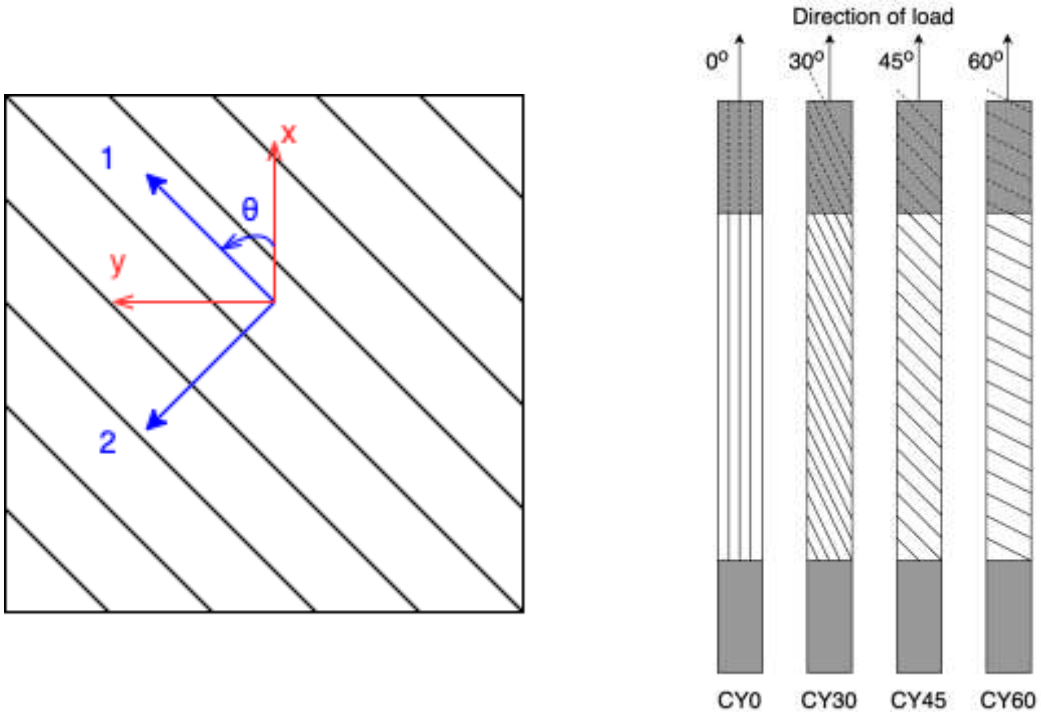

(a) (b)

Figure 3. (a) Global axes and material axes, (b) alignment of fiber for four different sets of the test sample

In an angled lamina, the stresses are applied at a certain angle with respect to the fiber direction. For angle ply lamina, stress is applied in accordance with the global coordinate system. The direction of load is referred to as the X-axis and the direction perpendicular to the load is referred to as the Y-axis.. (Figure 3 (a)). The angle between material and global axes is denoted by θ and is chosen as positive as the fiber turns out in a counterclockwise direction. The direction of fibers for four different sets of samples can be seen in Figure 3 (b). When stress is applied in global axes, the relation between stress and strain is given by Equation (2).

$$\begin{bmatrix}\sigma_x\\ \sigma_y\\ \tau_{xy}\end{bmatrix}=\begin{bmatrix}\bar{Q}_{11} & \bar{Q}_{12} & \bar{Q}_{16}\\ \bar{Q}_{12} & \bar{Q}_{22} & \bar{Q}_{26}\\ \bar{Q}_{16} & \bar{Q}_{26} & \bar{Q}_{66}\end{bmatrix}\begin{bmatrix}\varepsilon_x\\ \varepsilon_y\\ \gamma_x\end{bmatrix} \tag{2}$$

Here $[\bar{Q}\,]$are the transformed, reduced stiffness matrix and each element of $[\bar{Q}\,]$ can be calculated by Equation (3)

$$\begin{aligned}
\bar{Q}_{11} &= Q_{11}c^4 + Q_{22}s^4 + 2(Q_{12}+2Q_{66})s^2c^2,\\
\bar{Q}_{12} &= (Q_{11}+Q_{22}-4Q_{66})s^2c^2 + Q_{12}(s^4+c^4),\\
\bar{Q}_{22} &= Q_{11}s^4 + Q_{22}c^4 + 2(Q_{12}+2Q_{66})s^2c^2,\\
\bar{Q}_{16} &= (Q_{11}-Q_{12}-2Q_{66})c^3s - (Q_{22}-Q_{12}-2Q_{66})s^3c,\\
\bar{Q}_{26} &= (Q_{11}-Q_{12}-2Q_{66})cs^3 - (Q_{22}-Q_{12}-2Q_{66})s^3c,\\
\bar{Q}_{66} &= (Q_{11}+Q_{22}-2Q_{22})s^2c^2 + Q_{66}(s^4+c^4),
\end{aligned} \tag{3}$$

Here it can be seen that each element of the transformed, reduced stiffness matrix is related to four stiffness elements ($Q_{11}, Q_{12}, Q_{22}, Q_{66}$) and the constants $c = \cos\theta \ and \ s = \sin\theta$. The four stiffness elements are functions of four engineering constants ($E_1, E_2, \upsilon_{12}, \upsilon_{21}$) and can be seen in Equation (4).

$$Q_{11} = \frac{E_1}{1-\upsilon_{21}\upsilon_{12}},$$
$$Q_{12} = \frac{\upsilon_{12}E_2}{1-\upsilon_{21}\upsilon_{12}},$$
$$Q_{22} = \frac{E_2}{1-\upsilon_{21}\upsilon_{12}}, \quad (4)$$
$$Q_{66} = G_{12},$$

3. RESULTS

In order to see the response of Hooke's law on a lamina, first, CY0 samples are tested and analyzed with Hooke's law. Since CY0 samples are only composed of fibers parallel to the applied load, Hooke's law and experimental results are expected to converge to each other better when compared to angle ply lamina. Indeed, the results obtained to confirm this assumption. The experimental stress-strain curves and the response of Hooke's law for CY0 samples can be seen in Figure 4.

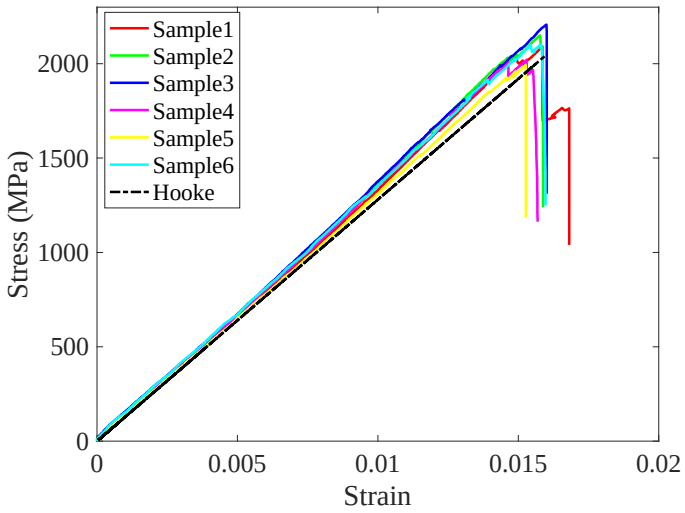

Figure 4. Experimental and Hooke's law stress-strain curve for CY0 samples.

Once it is confirmed that Hooke's law converges for the lamina with fibers aligned only in a direction parallel to load, Hooke's law is applied to the angle-ply laminate. The first angle ply lamina that the appropriate response of Hookes' law is examined to experimental results is the CY30. Although six different coupons are prepared for the test of CY30, only two of them are being tested successfully. The underlying reason behind this problem is the brittleness of CY30 samples. As mentioned in the "Materials and Sample Preparation section," the CY30 samples are so brittle that the extraction of samples is being done with a water jet. That brittleness also does not allow to conduct of tensile tests successfully. The stress-strain curves produced with Hooke's law and experiment can be seen in Figure 5 for CY30. Although Hooke's law produces results that agree with the experiment for CY0, the

situation is entirely different for CY30 samples. Hooke's law produces relatively close results with the experiment for small strain values while significantly deviating from experimental results for the high strain values. These relatively small strain values do not make sense in applying Hooke's law to the angle ply lamina. These small strain values are mostly not applicable, and an angle ply lamina can undergo higher strain values than Hooke's law.

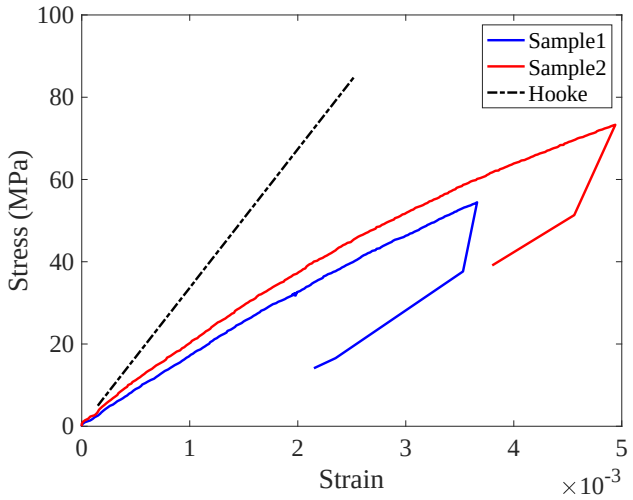

Figure 5. The comparison of stress-strain curves with Hooke's law for CY30 samples

Test coupons with 45 ° fibers, CY45, are tested to see that the error observed in CY30 specimens can be reduced. When the results obtained by Hooke's law and experiments are compared for CY45, it is clearly seen that in Figure 6, Hooke's law does not correlate with the experimental finding. Even though five different specimens are tested experimentally, and all indicate the same stress-strain curve, Hooke's law finding deviates from all the experimental stress-strain curves.

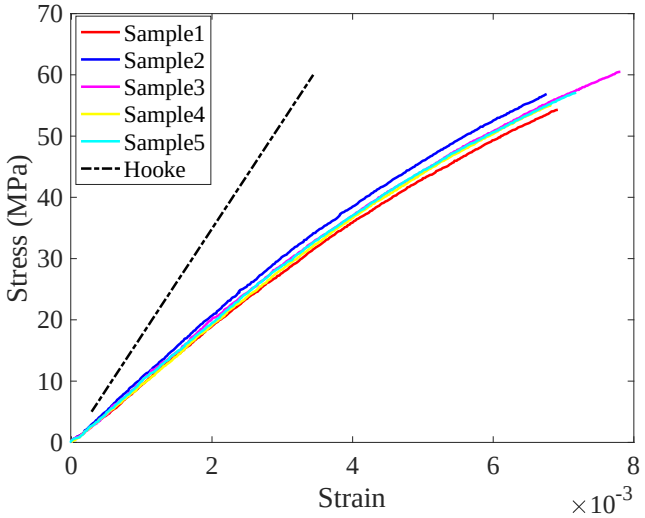

Figure 6. The comparison of stress-strain curves with Hooke's law for CY45

The last attempt is made with CY60 samples to see whether Hooke's law applies to the angle ply lamina. As shown in Figure 7, Hooke's law does not converge the experimental stress-strain curves for CY60

specimens. However, it can be seen from Figure 7 that Hooke's law produces better results for CY60 samples when compared to those of CY30 and CY45.

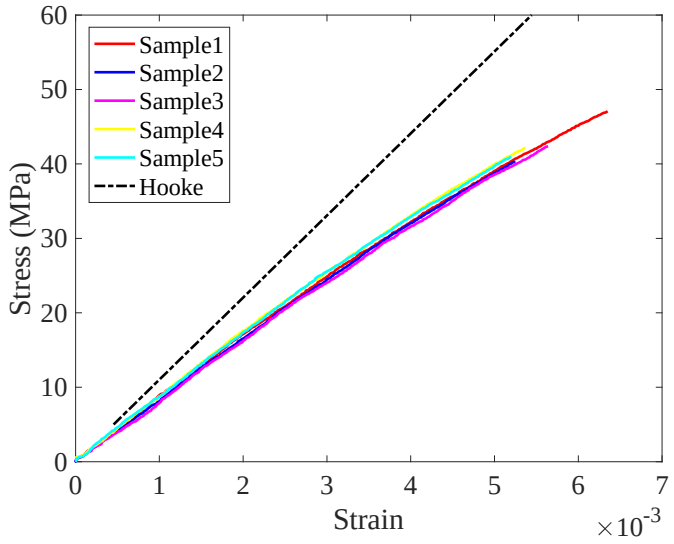

Figure 7. The comparison of stress-strain curves with Hooke's law for CY60

Four types of samples are being tested in this study, and their fracture images are taken and depicted in Figure 8. It can be seen from Figure 8 (a) that samples containing fibers parallel to load failed as if fibers exploded due to extensive splitting, and it is observed that the fibers are fringed. It is not possible to observe a clear fracture plane as can be observed from the other fractured samples. Figure 8 (b), (c), (d) represent the failed specimens from the CY30, CY45, and CY 60 batch, respectively. CY30, CY45, and CY 60 specimens indicate clear fracture planes and fracture angles based on the direction of fibers. It can be seen from Figure 8 (b-d) that as the angle of fibers with respect to load increases, the angle of the fracture plane also increases.

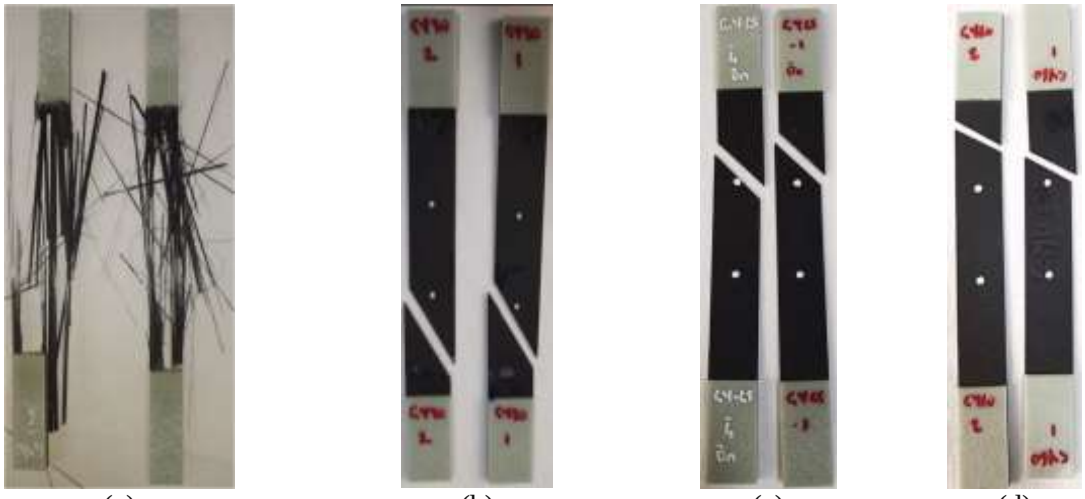

Figure 8. Fractured samples after tensile test; (a) CY0, (b) CY30, (c) CY45, (d) CY60

4. DISCUSSION

Herein, four different aerospace-grade angle ply laminates are produced with an autoclave manufacturing method, tested experimentally in ISO 17025 and AS 9100 certified laboratories, and the application of Hooke's law to the experimental results is analyzed. It is found that the correlation of Hooke's law with experimental results is very well for a laminate composed of only unidirectional fibers. When Hooke's law is applied for an angle ply lamina, there is a significant amount of deviation from the experimental stress-strain curves.

The autoclave used in test plate production is located at Advanced Composite Manufacturing (ACM) laboratory at Sabanci University Integrated Manufacturing Research and Application Center (SU IMC). The vacuum, pressure, and thermocouples found on the autoclave have all the annual calibrations and verifications, and the ACM is an AS 9100-certified laboratory. Technical personnel produces the test plates based on the written order, and all the technicians have the necessary training and at least two years of lamination experience to complete the given jobs accurately.

The Universal Testing Machine (UTM), mechanical and optical extensometers used in the mechanical testing of test coupons are also located Mechanical Testing laboratory at Sabanci University Integrated Manufacturing Research and Application Center (SU IMC). The UTM machine and extensometers also have annual calibration and verification after every six months. The mechanical testing laboratory is ISO 17025 and AS9100 certified. All the technical personnel who contribute to mechanical tests have the necessary training and experience.

Even though all the manufacturing and testing are done by qualified personnel and calibrated equipment in certified laboratories, the significant amount of divergence results produced by Hooke's law compared with the experimental results indicates the insufficiency of the theorem. According to obtained results for angle ply lamina, Hooke's law always overestimates the experimental results. This overestimation behavior of Hooke's law can be attributed to its linear elastic estimation of the relation between stress and strain. For the angle ply lamina, as the stress increases, the linear relationship between the stress and strain diminishes due to increased shear stress. The reason behind the deviation between Hooke's law predicted results and experimental results is the factor of an interface failure, which Hooke's law does not account for in the calculation.

5. CONCLUSION

Herein, the applicability of Hooke's law to the angle-ply laminate is analyzed. First, four different materials constants for unidirectional lamina, namely longitudinal elastic modulus (E_{11}), transverse elastic modulus (E_{22}), in-plane shear modulus (G_{12}), and major Poisson's ratio (υ_{12}) are measured. Then these measured material constants are fed into Hooke's law to investigate the appropriateness of Hooke's law for angle ply lamina. The following conclusions are drawn in this study:

1) The stress-strain curve produced by Hooke's law agrees well with the experimental stress-strain curve for unidirectional lamina.
2) However, the results generated by Hooke's law do not coincide well with the experimental results for angle ply lamina.
3) Hooke's law approaches the experimental stress-strain curve only for relatively small strains.
4) Therefore, the reliability of Hooke's law should be questioned for the angle-ply lamina, and this reliability problem should be considered when Hooke's law is taught in composite material courses at undergraduate and graduate levels.

ACKNOWLEDGMENTS

This work was partially supported by the Sabanci University Integrated Manufacturing Research (SU-IMC) and Application Center.

CONFLICT OF INTEREST

The authors stated that there are no conflicts of interest regarding the publication of this article.

REFERENCES

[1] Yilmaz C, Yildiz M. A study on correlating reduction in Poisson's ratio with transverse crack and delamination through acoustic emission signals. Polym Test 2017;63:47–53. https://doi.org/10.1016/j.polymertesting.2017.08.001.

[2] Yilmaz C, Akalin C, Gunal I, Celik H, Buyuk M, Suleman A, et al. A hybrid damage assessment for E-and S-glass reinforced laminated composite structures under in-plane shear loading. Compos Struct 2018;186:347–54. https://doi.org/10.1016/j.compstruct.2017.12.023.

[3] Yilmaz C, Akalin C, Kocaman ES, Suleman A, Yildiz M. Monitoring Poisson's ratio of glass fiber reinforced composites as damage index using biaxial Fiber Bragg Grating sensors. Polym Test 2016;53:98–107. https://doi.org/https://doi.org/10.1016/j.polymertesting.2016.05.009.

[4] Ali HQ, Emami Tabrizi I, Khan RMA, Tufani A, Yildiz M. Microscopic analysis of failure in woven carbon fabric laminates coupled with digital image correlation and acoustic emission. Compos Struct 2019;230:111515. https://doi.org/https://doi.org/10.1016/j.compstruct.2019.111515.

[5] Munoz V, Valès B, Perrin M, Pastor M-L, Welemane H, Cantarel A, et al. Damage detection in CFRP by coupling acoustic emission and infrared thermography. Compos Part B Eng 2016;85:68–75.

[6] Emami Tabrizi I, Alkhateab B, Seyyed Monfared Zanjani J, Yildiz M. Using digital image correlation for in situ strain and damage monitoring in hybrid fiber laminates under in-plane shear loading. Polym Compos 2021;n/a. https://doi.org/https://doi.org/10.1002/pc.26114.

[7] Saeedifar M, Saleh MN, El-Dessouky HM, Teixeira De Freitas S, Zarouchas D. Damage assessment of NCF, 2D and 3D woven composites under compression after multiple-impact using acoustic emission. Compos Part A Appl Sci Manuf 2020;132:105833. https://doi.org/https://doi.org/10.1016/j.compositesa.2020.105833.

[8] Strungar EM, Yankin AS, Zubova EM, Babushkin A V, Dushko AN. Experimental study of shear properties of 3D woven composite using digital image correlation and acoustic emission. Acta Mech Sin 2019:1–12.

[9] Khan RMA, Tabrizi IE, Ali HQ, Demir E, Yildiz M. Investigation on interlaminar delamination tendency of multidirectional carbon fiber composites. Polym Test 2020;90. https://doi.org/10.1016/j.polymertesting.2020.106653.

[10] Khan RMA, Saeidiharzand S, Emami Tabrizi I, Ali HQ, Yildiz M. A novel hybrid damage

monitoring approach to understand the correlation between size effect and failure behavior of twill CFRP laminates. Compos Struct 2021; 270: 114064. https://doi.org/https://doi.org/10.1016/j.compstruct.2021.114064.

[11] Evran S. Buckling temperature analysis of laminated composite plates with circular and semicircular holes. Eskişehir Tech Univ J Sci Technol A - Appl Sci Eng 2020;21:173–81.

[12] Ubaid J, Kashfuddoja M, Ramji M. Strength prediction and progressive failure analysis of carbon fiber reinforced polymer laminate with multiple interacting holes involving three dimensional finite element analysis and digital image correlation. Int J Damage Mech 2014;23:609–35.

[13] Hara E, Yokozeki T, Hatta H, Ishikawa T, Iwahori Y. Effects of geometry and specimen size on out-of-plane tensile strength of aligned CFRP determined by direct tensile method. Compos Part A Appl Sci Manuf 2010;41:1425–33. https://doi.org/https://doi.org/10.1016/j.compositesa.2010.06.003.

[14] Nicoletto G, Anzelotti G, Riva E. Mesoscopic strain fields in woven composites: experiments vs. finite element modeling. Opt Lasers Eng 2009;47:352–9.

[15] Tabrizi IE, Khan RMA, Massarwa E, Zanjani JSM, Ali HQ, Demir E, et al. Determining tab material for tensile test of CFRP laminates with combined usage of digital image correlation and acoustic emission techniques. Compos Part A Appl Sci Manuf 2019; 127. https://doi.org/10.1016/j.compositesa.2019.105623.

[16] Akın Ataş Oİ. Experımental characterisation and prediction of elastic properties of woven fabric reinforced textile composıte laminates. Eskişehir Tech Univ J Sci Technol A - Appl Sci Eng 2018;19:660–70.

[17] Merve Çobanoğlu Fahrettin Öztürk REE. Thermoforming process parameter optimization of thermoplastic pekk/cf and PPS. Eskişehir Tech Univ J Sci Technol A - Appl Sci Eng 2021;22:51–8.

[18] Massarwa E, Emami Tabrizi I, Yildiz M. Mechanical behavior and failure of glass/carbon fiber hybrid composites: Multiscale computational predictions validated by experiments. Compos Struct 2021;260:113499. https://doi.org/https://doi.org/10.1016/j.compstruct.2020.113499.

[19] Philippidis TP, Theocaris PS. The Transverse Poisson's Ratio in Fiber Reinforced Laminae by Means of a Hybrid Experimental Approach. J Compos Mater 1994;28:252–61. https://doi.org/10.1177/002199839402800304.

[20] Lim T-C. Coefficient of thermal expansion of stacked auxetic and negative thermal expansion laminates. Phys Status Solidi 2011;248:140–7. https://doi.org/https://doi.org/10.1002/pssb.200983970.

[21] Parnas L, Katırcı N. Design of fiber-reinforced composite pressure vessels under various loading conditions. Compos Struct 2002;58:83–95. https://doi.org/https://doi.org/10.1016/S0263-8223(02)00037-5.

[22] Vnučec Z. Analysis of the laminated composite plate under combined loads. 5th Int. Sci. Conf. Prod. Eng., 2005, p. 143–8.

[23] Migliaresi C. Chapter I.2.9 - Composites. In: Ratner BD, Hoffman AS, Schoen FJ, Lemons

JEBT-BS (Third E, editors., Academic Press; 2013, p. 223–41. https://doi.org/https://doi.org/10.1016/B978-0-08-087780-8.00024-3.

[24] Kaw AK. Mechanics of composite materials. CRC press; 2005.

[25] Öchsner A. Macromechanics of a Lamina BT - Foundations of Classical Laminate Theory. In: Öchsner A, editor., Cham: Springer International Publishing; 2021, p. 11–39. https://doi.org/10.1007/978-3-030-82631-4_2.

[26] Ali HQ, Yilmaz Ç, Yildiz M. The effect of different tabbing methods on the damage progression and failure of carbon fiber reinforced composite material under tensile loading. Polym Test 2022:107612. https://doi.org/https://doi.org/10.1016/j.polymertesting.2022.107612.

[27] Standard Test Method for Tensile Properties of Polymer Matrix Composite Materials n.d.

[28] Materials AS for T and. Standard Test Method for In-plane Shear Response of Polymer Matrix Composite Materials by Tensile Test of a ±45 ° Laminate. ASTM International; 2007.